J. Mater. Environ. Sci. 5 (6) (2014) 1758-1769
ISSN : 2028-2508
CODEN: JMESCN

Preparation and characterization of activated carbon from date pits by chemical activation with zinc chloride for methyl orange adsorption

Khaled Mahmoudi, Noureddine Hamdi*, Ezzeddine Srasra
Laboratory of Physicochemical of Minerals Materials and its Applications
National Centre of Research in Materials Sciences (CNRSM) B.P.73 – 8020. Soliman Tunisia

Received 7 Dec 2013, Revised 7 July 2014, Accepted 7 July 2014
** Corresponding author. Email: hamdinoureddine@yahoo.fr*

Abstract
Natural material such as date pits have been used as precursor for activated carbon, using zinc chloride as activating agent. The effect of preparation conditions on the produced activated carbon characteristics as an adsorbent was investigated. The performance of the synthesized carbon was characterized by N_2 adsorption–desorption isotherms, BET equations, SEM and FTIR. The optimum conditions for carbon preparation are as follows: activation temperature, 400°C; activation time, 2 hours; mass ratio of activating agent is about 2:1. The specific surface area attains 1380 m^2/g and the pore volume is 0.91 cm^3/g. The pore structure of the activated carbon is mainly composed of micropore the ratio is of order of 50%. The surfaces of carbon are dominated by the carbonyl and hydroxyl group. The activated carbon was utilized as adsorbent to remove methyl orange (MO) from aqueous solutions. Batch experiments were conducted to study the effects pH, contact time and initial MO concentration on the adsorption capacity. The equilibrium experimental data were fitted by the Langmuir and Freundlich models. The better fit was showed with the Langmuir isotherm equilibrium model.

Key words: Activated carbon, Date pits, zinc chloride, adsorption, methyl orange.

1. Introduction
Activated carbon is one of the most widely used materials in water treatment because of its exceptional adsorbent properties, high surface area and microporosity good corrosion resistance. In general, preparation of activated carbon is commonly classified into chemical activation and physical activation. Since chemical activation usually takes place at a lower temperature and a shorter time is needed for activating the materials, the chemical activation is lower energy cost.
The most studied chemical activation parameters are time, temperature, and impregnation ratio (activating agent/precursor). The activation time has little influence on the process (1 and 2 h are common in most works) [1-3]. In contrast, activation temperature and impregnation ratio are very important. Generally, the increase in activation temperature leads to an increase in surface area and a decrease in yield. The impregnation ratio shows a similar behavior; however, the yield decrease is less pronounced and larger surface areas are obtained. ACs with high surface area and considerable yields are obtained at activation temperatures around 500°C [4-6].
In chemical activation, the main activating agents used are $ZnCl_2$ [7-11], KOH [12], NaOH [13], K_2CO_3 [14, 15] and H_3PO_4 [16-18]. Taking their environmental effect and chemical recovery into consideration, $ZnCl_2$ is most preferred.
Severals researchers have reported the preparation of chemically activated carbons from many kinds of raw materials, as for example from peanut [19, 20] and lignine [21], sawdust [22-24], rice [25,26], cherry stones [27], bagasse fly ash [28], peach stones [29] olive-waste cakes [30], olive stones [31], date stones [32,33] dates pits [34, 35], were chosen to prepare activated carbon successfully due to high wood fiber content. A high surface area and an adequate pore size distribution are very important for the activated carbon to perform well in a particular application. However, activated carbons with similar porous characteristics may show a very different adsorption capacity with the same adsorbates. This is because the porous texture influences the optimization of the adsorption capacity of activated carbons.

The nature and the amount of the surface functional groups existing in the activated carbon surface must also be taken into account. Surface functional groups of carbon materials directly depend on the presence of heteroatoms such as hydrogen, oxygen, nitrogen etc. and inorganic ash components that may come from the carbon precursor or activating agent.
The main object of this study was the production of a higher value activated carbon product from date pits via chemical activation with chloride zinc. In addition, the surface chemistry of activated carbon samples was investigated using BET, SEM and FTIR spectroscopy. This was carried out to gain more insight into the changes occurring in the surface chemistry of the activated carbons with different temperatures. This paper contains again the effects of the operating variables (pH of the solution, initial concentration of solute and contact time) on the performance of activated carbon in adsorbing methyl orange.

2. Materials and methods

The starting date pits were washed several times with water and then dried at 423 K. The dried pits were crushed and sieved, the fraction of particle size between 0.5 and 1.0 mm well be used for the preparation of activated carbon.
The activated carbon sample was produced by chemical activation with zinc chloride (99%) and date pits, provided from Tunisia. Date pits were added to $ZnCl_2$ grains with an impregnant / precursor mass ratio of 2 and were mixed until the total homogeneity. The mixture of natural date pits and activated reagent ($ZnCl_2$) was heated up to different final carbonization temperatures in the same furnace at the rate of 10°/min (the activation temperature was varied over the temperature range of 300–500°C).
The low temperature ramp rate was used to minimize the temperature difference between mixture and furnace, to provide sufficient activation time and to avoid a rapid decomposition of the sample. The samples were cooled below 323 K before removing from the furnace. After cooling to room temperature, the activation mixture was washed several times with hot distilled water to remove residual chemical activating agent.
After the washing process, the sample was dried at 80°C in a vacuum oven for least than 2 h, in order to obtain the activated carbon.
The pore size distribution, surface area (S_{BET}), micro pore volume (V_{micro}) and total pore volume (V_{TOT}) of the produced carbon were determined from the nitrogen adsorption-desorption isotherm at 77K using a Quantachrome Autosorb 1-MP. S_{BET} is determined by Brauner-Emmet-Teller (BET) method [36] and t-plot method was used to estimate the volumes of micropores and micropore surface area. The total pore volume (Vp) was estimated from the amount of nitrogen adsorbed at a relative pressure of P/P_o =0.97 and the average pore diameter was calculated from $D_p = 4V_p/S_{BET}$ [37].
The PZC is pH at which the surface has zero net charge, known as pH_{pzc}, is characteristic of amphoteric surfaces and is determined by the type of surface sites on solids and their structures. The samples of powders (0.15 g) with 50 mL of 0.01 M NaCl solution were shaken in the bottle for 48 h. The initial pH values were adjusted (in the pH range from 3.5 to 10) by adding a small amount of HCl or NaOH solution keeping the ionic strength constant. The final pH was measured after 48 h under agitation at room temperature. The point of zero charge of the adsorbent (pHpzc) is the point where the curve pH_{final} versus $pH_{initial}$ crosses the line $pH_{initial} = pH_{final}$ [38, 39].
The morphology of raw material and activated carbons produced from date pits were examined using scanning electron microscopy (Philips Fei Quanta 200).
Chemical characterization was carried out by FTIR spectroscopy in order to identify the functional groups at the surface of carbon materials. The infrared transmission spectra were recorded with a Perkin Elmer spectrometer, from 400 to 4000 cm^{-1}, using the KBr wafer technique. 32 hundred scans were taken with a 2 cm^{-1} resolution. Wafers were prepared from the mixture of 1 mg of the sample and 200 mg of KBr. This mixture was compacted in a manual hydraulic press.
The amounts of acidic functional groups were determined by Boehm's method of titration with basic solutions of different base strengths ($NaHCO_3$, Na_2CO_3, NaOH, C_2H_5ONa) [40, 41]. This was achieved by accurately weighing 1.00g sample into four conical flasks with stopper.
For this purpose the samples were agitated for at least 16 h with 0.05 N solutions of four bases. The amount of Na^+ ions remaining in the solution is determined by adding an excess of standard HCl and back-titration. The basic groups contents of the oxidized samples are determined with 0.05 N HCl [41, 42].
The batch sorption studies were conducted in a set of 250 ml Erlenmeyer flasks containing 0.10 g adsorbent and 200 mL dye solutions with various initial concentrations (50, 250, 500, 750, 850, and 1000 mg/L). The flasks were agitated in an isothermal shaker at 200 rpm and 30 °C until the equilibrium was reached. Dye

concentrations in the supernatant solutions were measured by a double beam UV–vis spectrophotometer (Perkin-Elmer, Model UV Lambda 20) at 460 nm MO uptake at equilibrium, q_e (mg/g), was determined by:

$$q_e = \frac{(C_0 - C_e).V}{W}$$

where C_0 and C_e (mg/L) are the liquid-phase concentrations of dye at initial and equilibrium, respectively. V (L) is the volume of the solution, and W (g) is the mass of adsorbent used. The effect of pH on dye removal was examined by varying the pH of the solution from 2 to 12, with initial dye concentration of 1000 mg/L, DPAC dosage of 0.10 g/500 mL and adsorption temperature of 30°C. The initial pH of the dye solution was adjusted by addition of 0.10 M solution of HCl or NaOH.

The equilibrium data were fitted using Langmuir and Freundlich isotherm models [43,44].

Langmuir isotherm assumes monolayer adsorption onto a surface containing a finite number of adsorption sites. The linear form of Langmuir isotherm equation is derived as Langmuir, 1916 [45]:

$$\frac{C_e}{q_e} = \frac{1}{Q_0 K_L} + \frac{1}{Q_0} C_e$$

where Q_o (mg/g) and K_L (dm^3/g) are Langmuir constants related to adsorption capacity and rate of adsorption.

Freundlich isotherm assumes heterogeneous surface energies, in which the energy term in Langmuir equation varies as a function of the surface coverage. The well-known logarithmic form of the Freundlich isotherm is given by Freundlich, 1906 [46]:

$$Ln\ q_e = Ln\ K_F + \frac{1}{n} Ln\ C_e$$

where K_F (mg/g) (L/mg) and 1/n are the Freundlich adsorption constant and a measure of adsorption intensity.

The procedure of adsorption kinetic was identical to adsorption equilibrium where the aqueous samples were withdrawn at different time intervals and the concentrations of MO were similarly measured. The amount of adsorption at time t, qt (mg/g), was calculated by:

$$q_t = \frac{(C_0 - C_t)V}{W}$$

where C_t (mg/l) is the liquid-phase concentrations of dye at time, t. When adsorption is preceded by diffusion through a boundary, the kinetics in most systems follow pseudo-first-order equation. The first-order expression of (Lagergen, 1898) [47] based on solid capacity is defined as:

$$ln\left(\frac{q_e}{q_e - q_t}\right) = \frac{k_1}{2.303} t$$

where k_1 (1/h) is the adsorption rate constant. Contrary to pseudo first- order equation, pseudo second-order equation (Ho, 1998) [48] predicts the behavior over the whole range of adsorption and represented by:

$$\frac{1}{(q_e - q_t)} = \frac{1}{q_e} + k_2 t$$

where k_2 (g/mg h) is the adsorption rate constant of pseudo second-order equation.

3. Results and discussion

3.1. Samples characterization

The activation temperatures play an important role in determining the porous structure and the surface area. Activation temperature determines the devolatilisation and activation reaction rates of the carbon. Activation temperature will also affect the quality of activated carbon from date pits. It is known that theoretically the function of the total surface area and pore volume will increase and then decrease with temperature. Since at the beginning of the activation process, low burn-off only allows partial pore development, the increase of temperature will allow better micropore development and results in larger surface areas and pore volume. However, with prolonged activation, micropore widening followed by collapsing occurred to form meso or macropore, this effect will be cycling throughout the whole activation. Many researchers have linked the surface area and total pore volume of the activated carbon with the degree of burn-off [49]. They suggested that the activation time produced a positive effect on the BET surface area as more porosity was developed in the carbon [50].

$$\textbf{Acivation burn} - \textbf{off}\ (\%) = \left\{100 - \left[\frac{\textbf{mass after activation(g)}}{\textbf{original mass (g)}}\right] * 100\right\}$$

Fig. 1 gives the nitrogen adsorption isotherms at 77K of the activated carbons produced at the carbonization temperatures of 300, 400, 450 and 500°C. According to IUPAC classification, these isotherms are of Type I, which represents dense micropore structures. Moreover, Fig. 1 shows that with increasing carbonization temperature there is an upward trend in adsorption, that is to say, the surface area increases. Above 400C, the amount of adsorbed nitrogen by ADPs decreases. Surface area increases according to the temperature; above 400°C, the surface area decreases.

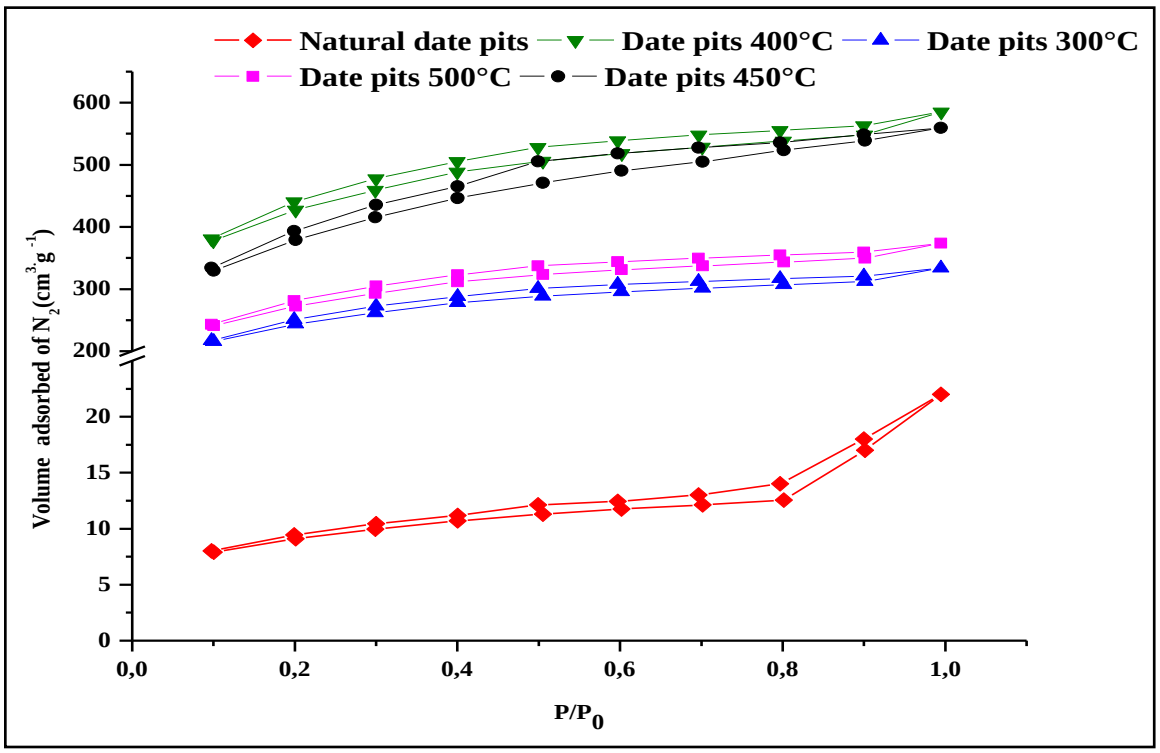

Figure 1: Nitrogen adsorption isotherms

Fig. 2 gives variations of the S_{BET} and micropore surface areas as a function of carbonization temperatures of activated carbons; Fig. 3 shows variations in the total and micropore volumes and Fig. 4 variations in pore size distribution as function of carbonization temperature.

For ADPs, a carbonization temperature of 400°C yielded the higher BET surface and micropore areas of 1380 m^2/g and 1245 m^2/g, respectively (Fig. 2).

For the ADPs activated carbons, this value is an upward trend up to a carbonization temperature of 400°C as compared to an increase beyond this temperature. In contrast, above this temperature, the S_{BET}, micropore surface and micropore volume were decrease (Fig. 2 and 3).

Similarly, for ADPs, there was an increase for total pore and micropore volume up to 400°C followed by a decrease beyond thereafter. For DP 400°C, the total pore and micropore volume are 0.9 cm^3/g and 0.49 cm^3/g.

The total pore and micropore volume of ADP 300°C were found to be 0.4 cm^3/g and 0.3 cm^3/g and those for ADP 450°C 0.85 cm^3/g and 0.45 cm^3/g, respectively. In contrast, for ADP 500, the values were 0.5 cm^3/g and 0.3 cm^3/g (Fig. 3). The BET and micropore surface areas of DP 300°C are 600 m^2/g and 520 m^2/g (Fig. 3). The BET and micropore surface areas of DP 450°C were established to be 1260 m^2/g and 1150 m^2/g and those of DP 500°C 700 m^2/g and 540 m^2/g, respectively. DP 300°C had a micropore surface area of 86.6 %, DP 400°C 90.21%, DP 450C°C 85.31% and DP 500°C 77.14%. The total pore volume was established to be 0.4 cm^3/g for DP 300°C, 0.85 cm^3/g for DP 450°C and 0.5cm^3/g for DP 500°C.

Figure 4 shows the SEM images of the natural and activated date pits prepared by $ZnCl_2$ activation. The natural sample has a very rough surface, an intact external structure where the caking and agglomeration of the carbonaceous aggregates was not observed. On the other hand, Fig. b shows the structure of a chemically activated date pits at carbonization of 400°C. We can observe, the external surface of the chemically activated date pits is full of cavities.

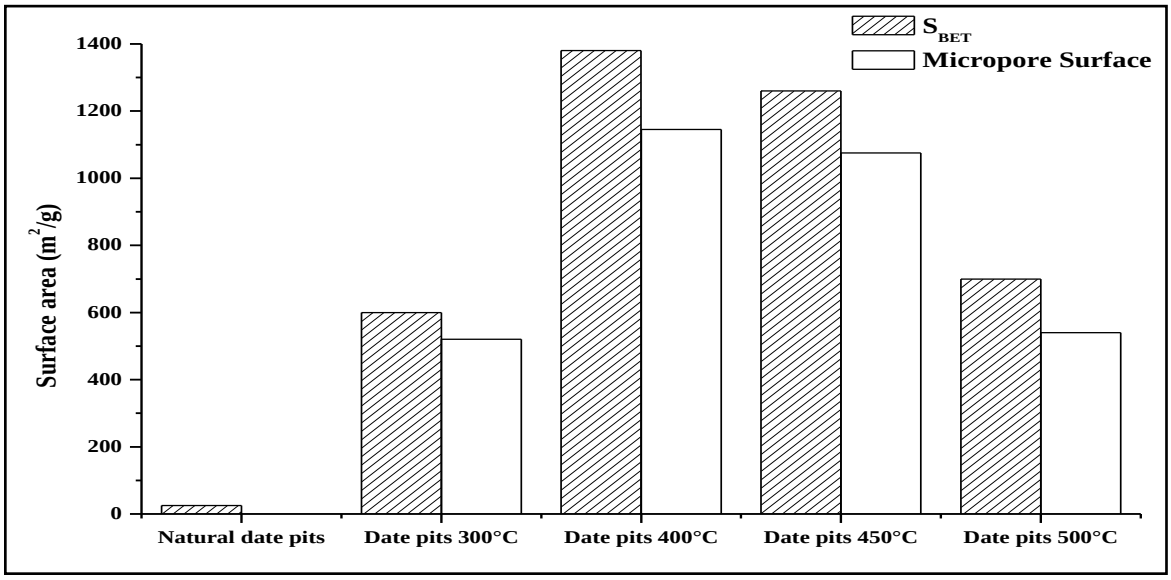

Figure 2: Variations in the BET and micropore surface areas of activated carbon at different temperature

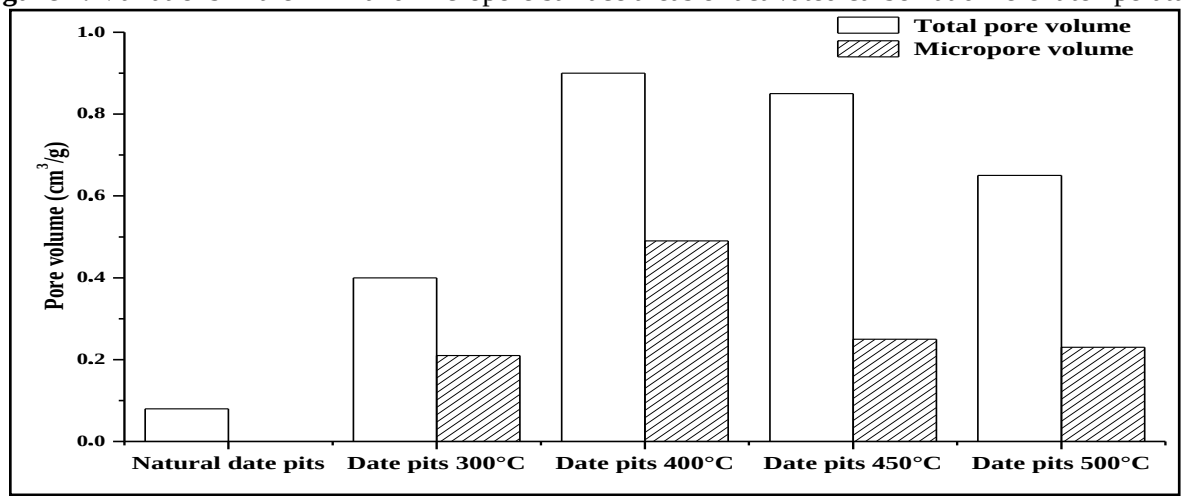

Figure 3: Variations in the pore volume of activated carbon at different temperature

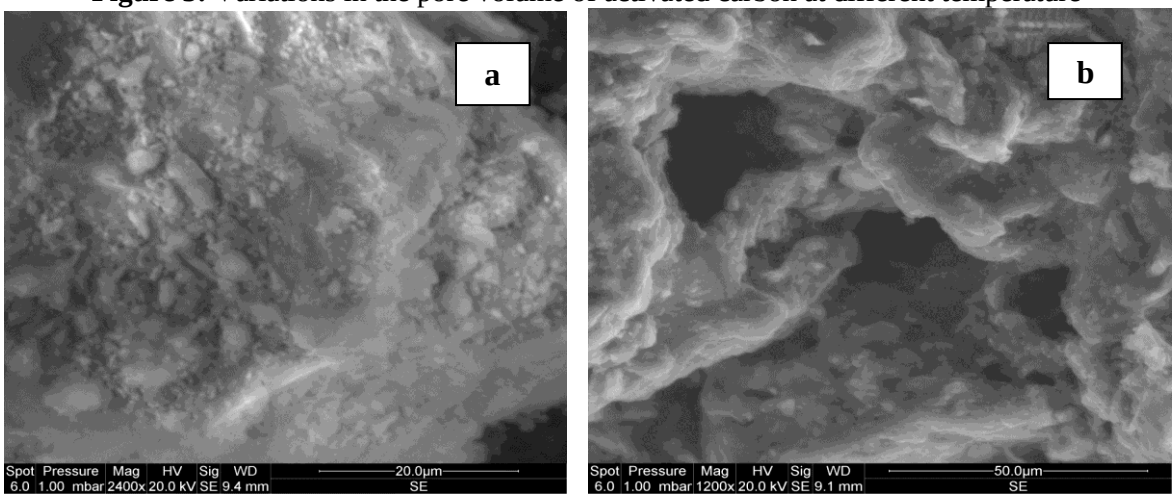

Figure 4: a Natural date pits at ambient temperature, **b** SEM of activated date pits prepared by $ZnCl_2$ activation with carbonization at 400°C for 2 h

In this work, infrared spectroscopy was used to obtain information about the chemical structure and functional groups of the raw material and the prepared activated carbon at different temperatures.

FT-IR spectra as shown in Fig. 5 present the development of surface textures of the D.P.N, DP300, 400, 450 and D.500. According to the literatures, it was found that D.PN presents the IR band around 3400cm^{-1} assigned to –OH vibration al stretching of hydroxyl groups. Bond at 1623cm^{-1} is the characteristic of the C= O stretching vibration of carbonyl groups.
Bond occurring at 1400 cm^{-1} ascribed to oxygen functionalities such as highly conjugated C=O stretching, C–O stretching in carboxylic groups, and carboxylate moieties.
Moreover, FT-IR spectra of D.P400, 400, 450°C and DP 500°C showed the decreasing of intensity of aliphatic bands around 2923 and 2855cm^{-1}, the IR band around 1623cm^{-1} assigned to stretching C=O of lactonic and carbonyl groups, a relative intense IR band at about 1033 cm^{-1} corresponding to C–O stretching in acids, alcohols, phenols, ethers and esters and the IR band located at 610cm^{-1} attributing to in-plane ring deformation [51, 52].
The main surface functional groups present were presumed to be phenols, carboxylic acids (or carboxylic anhydrides if they are close together) and carbonyl groups (either isolated or arranged in quinone-like fashion), all of which are typical acidic functional groups [53]. The surface of the date pits adsorbent could be proposed as follows.

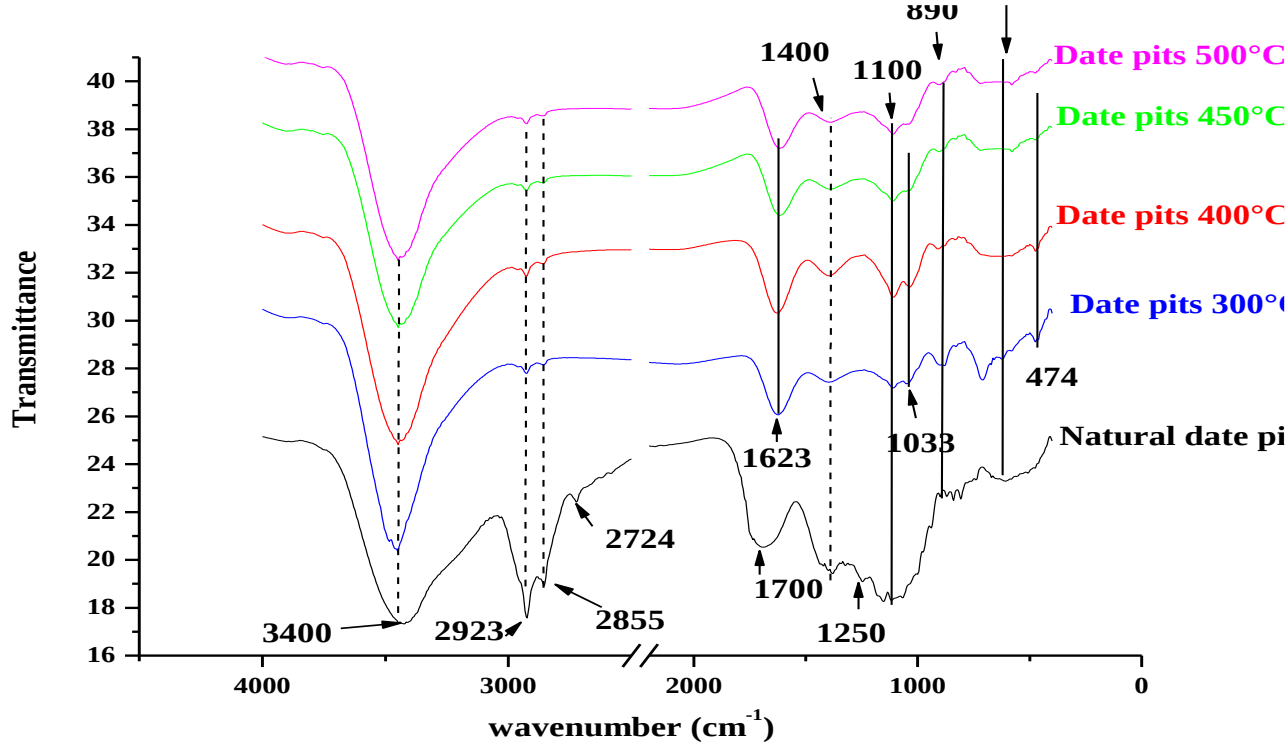

Figure 5: FTIR spectra of raw date pits and adsorbents prepared by chemical and thermal activation

The amount of acidic functional groups determined by Boehm method and the result is shown in Table1. It is apparent that the activation temperature has an influence on functional groups of prepared carbon. With the increasing of activation temperature, the amount of carboxylic groups and phenolic groups was increased from 1 to 3.8 mmol/g and 0.9 to 1.55 mmol/g while the amount of carbonyl groups was decreased from1.82 to 0.72 mmol/g. i.e. from DPN to DP400°C. A possible explanation for this could be that the carbonyl groups as a result of activation process.
As the surface acidity of carbon increased by chloride zinc activation, its pHpzc was lowered, whereas heat activation in a 400°C led to the higher value. pHpzc is closely related to the change of acidic or basic properties of the carbon.

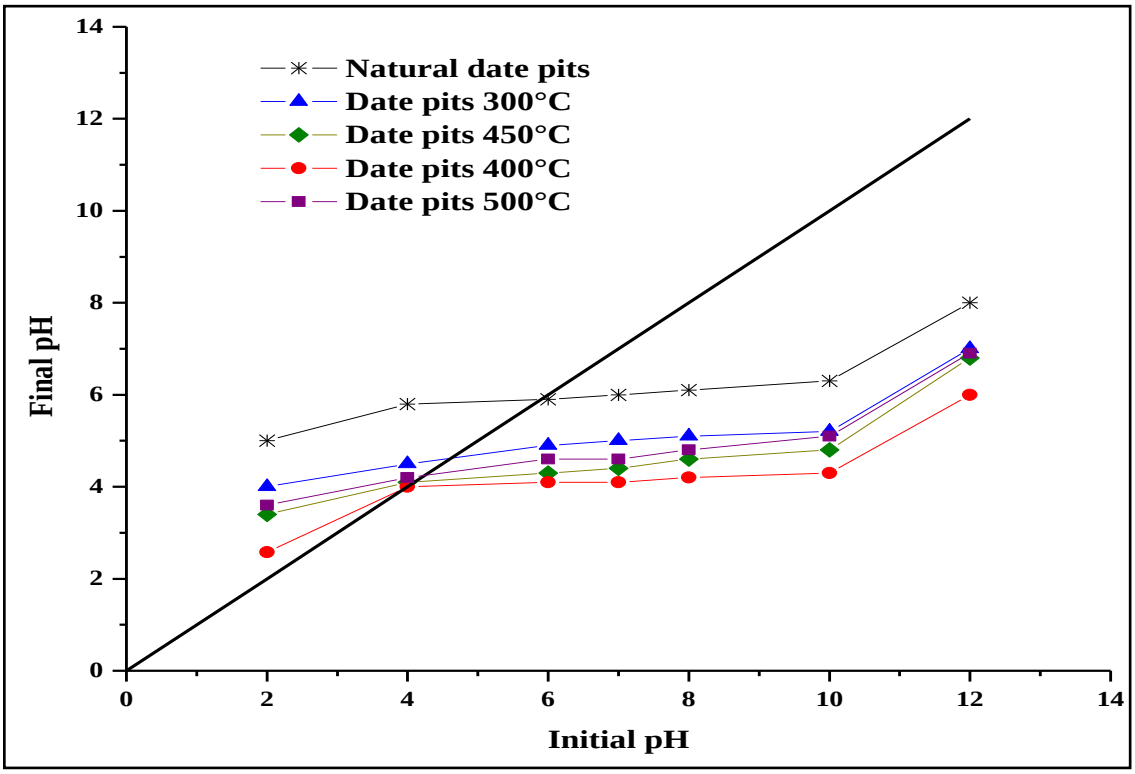

Figure 6: PZC of activated carbon

The points of zero charge of activated carbon at different temperatures are shown in Table 1. Carbons DP300, DP400 and DP450 gave acid values; it is possibly because the date's pits activated carbons all went through activation with zinc chloride.

Table 1: Surface chemical properties of sample.

Adsorbents	Functions acids (mmol/g)				Function basic (mmol/g)	pH_{PZC}
	Carboxylic groups	Phenolic groups	Lactonic groups	Total acid		
D.P.N	1	0.9	0.6	2.5	1.82	5.9
D.P.300°C	2.7	1	0.11	3.81	1.08	4.8
D.P.450°C	2.43	1.2	1.3	4.93	1	4.2
D.P.400°C	3.8	1.55	0.55	5.9	0.72	4.01

3.2. Adsorption experiments

Fig.7 shows the effect of pH on the adsorption of MO onto natural date pits and corresponding activated carbon. The initial concentration of MO was 1000 $mg.L^{-1}$. The adsorption of dyes was strongly pH dependent. The highest MO adsorption capacity was experimentally observed at pH 3.5, this capacity drastically decreased for higher pH values. The reduction of MO removal at pH values about 3.5 may be ascribed to the increasing repulsive forces between surface functional groups of AC and MO, which mainly exists as anion form. A similar result was reported by Araceli Rodrigeuz et al. 2009 [54] for the adsorption of orange II (acidic dye) on activated carbon (F-400).

The effect of contact time on adsorption capacity of NDP and ACDP for MO is shown in Fig. 8. This figure shows that the adsorption capacity for MO increases with the increase of contact time, and the adsorption reached equilibrium in about 6 h. For activated carbon from date pits, an adsorption capacity of 302 mg/g is obtained at 6 h contact time, 0.5 g/L adsorbent dose and 9 and 3.5 pH value respectively for MO. But the maximum adsorption capacitie of NDP observed 27 mg/g for MO at 4h. This figure also shows that rapid increase in capacity for MO is achieved during the first 1 h.

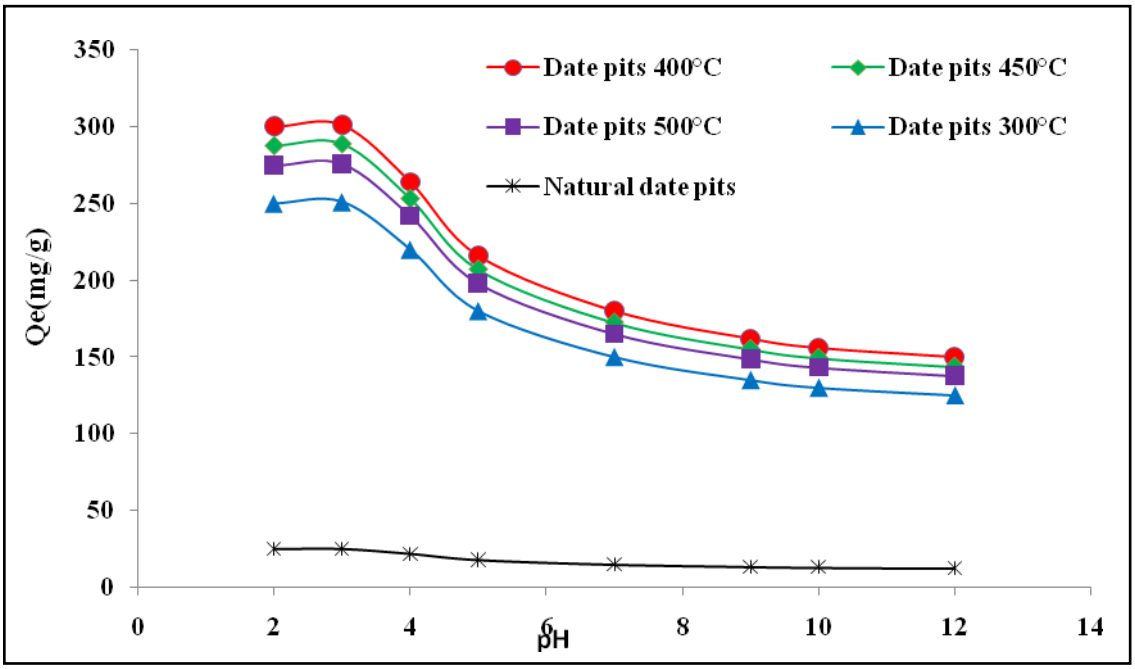

Figure 7: Effect of pH on the adsorption of methyl orange onto date pits and activated carbon

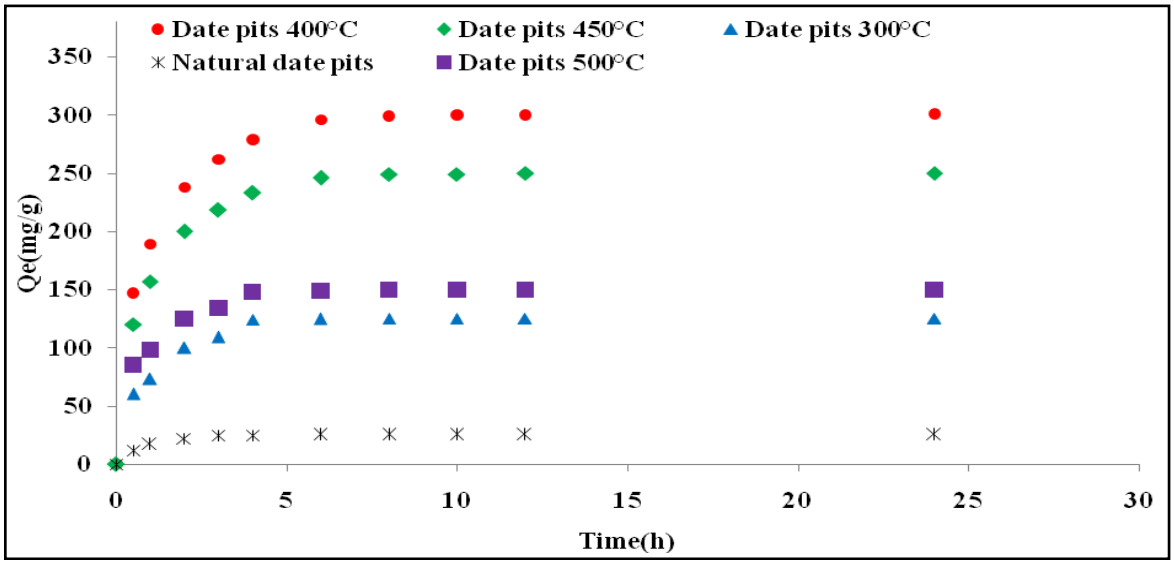

Figure 8: Effect of time for the adsorption of methyl orange on date pits before and after activation

The fast adsorption at the initial stage may be due to the higher driving force making fast transfer of MO ion to the surface of activated carbon particles and the availability of the uncovered surface area and the remaining active sites on the adsorbent.

The experimental kinetic data of MO, calculated from Eq. (1), were correlated by tow kinetic models: pseudo-first order and pseudo-second.

The calculated constants of the tow kinetic equations along with R^2 values of MO concentration are presented in Table 2. The linear plot of $\ln(q_e - q_t)$ versus t (Fig. 9a) for pseudo-first order equation is of low R^2 values, as shown in Table 2.

Moreover, this table shows a large difference between the experimental and calculated adsorption capacity values Δq (%), indicating a poor pseudo-first order fit to the experimental data. High R^2 values are obtained for the linear plot of t/q_t versus t (Fig. 9b) for pseudo-second order equation, as shown in Table 2. It can be seen that the pseudo-second order kinetic model better represented the adsorption kinetics and there are well agreements between the experimental and calculated adsorption capacity values Δq (%) (Table 2). This suggests that the adsorption of MO on natural date pits and activated carbon follows second-order kinetics.

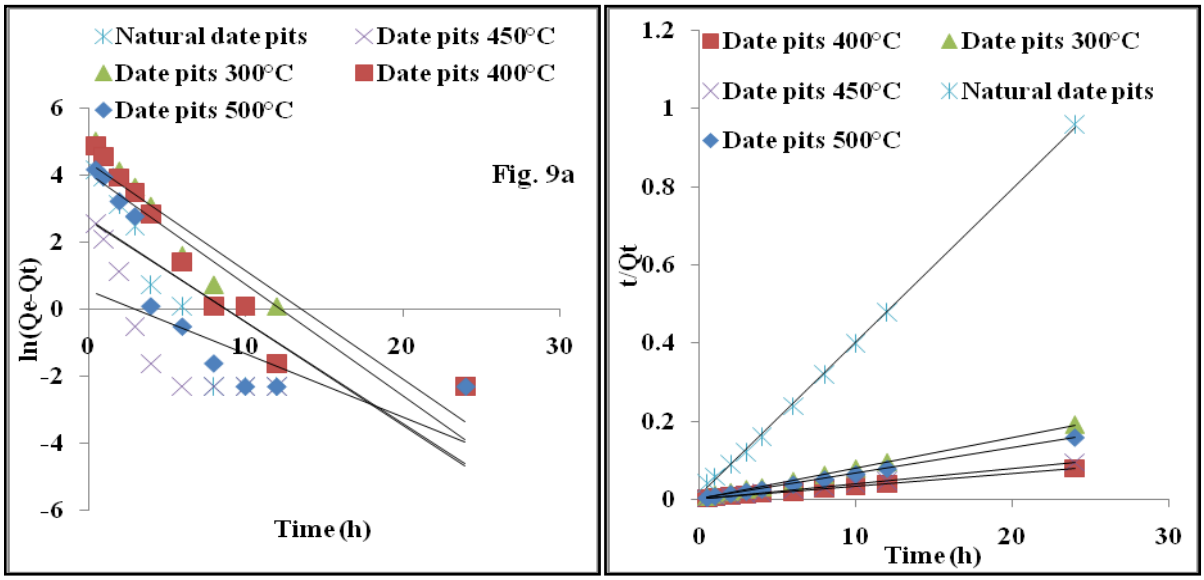

Figure 9: Pseudo- First order (Fig 9a) and pseudo-second order (Fig. 9b) kinetic plot for the adsorption of methyl orange on natural date pits before and after activation

Table 2: Kinetic parameters for the adsorption of MO onto natural date pits before and after activation at 25°C.

Adsorbents	$Q_{e.exp}$ (mg g^{-1})	First-order kinetic model			Second-order kinetic model		
		k_1 ($l.g^{-1}.h^{-1}$)	$Q_{e,calc}$ (mg g^{-1})	R^2	k_2 ($g.mg^{-1}.h^{-1}$)	$Q_{e,calc}$ (mg/g)	R^2
D.P.N	25	0.18	1.75	0.451	0.0105	25.44	0.999
D.P. 300°C	125	0.30	14.38	0.618	0.0033	125.20	0.999
D.P. 400°C	300	0,33	78.6	0,894	0,0015	312.5	0,999
D.P. 450°C	250	0.32	58	0.831	0.0018	263.15	0.999
D.P. 500°C	150	0.31	15.8	0.626	0.0022	153.84	0.999

From Table 2, the values of rate constant K_2 decrease with increasing initial concentration of MO. The reason for this behavior can be attributed to the high competition for the adsorption surface sites at high concentration which leads to higher sorption rates.

The mechanism of adsorption process is usually demonstrated by four steps: transport of adsorbate ions from bulk liquid to the liquid film or boundary layer surrounding the adsorbent, transport of adsorbate ions from the boundary film to the external surface of the adsorbent (surface diffusion), transfer of ions from the surface to the intra-particle active sites (pore diffusion), and adsorption of ions by the active sites of adsorbent. Because the first step is not involved with adsorbent and the fourth step is a very rapid process, they do not belong to the rate controlling steps.

The characteristic parameters of the different models as well as the correlation coefficients R^2 are listed in Table 3. As example, Fig.10 shows Langmuir and Freundlich isotherms, and the experimental data obtained at 25°C for methyl Orange. It can be seen that all models provided a good fit.

The correlation coefficients calculated for the Langmuir equation fitting are slightly lower than the ones obtained in the case Freundlich equation is used. However, we think that Langmuir describes better the experimental system, due to the experimental data reaches a saturation plateau at high C_e. This saturation tendency is not included in Freundlich model.

Table 3: Isotherms parameters obtained by Langmuir and Freundlich models for removal of MO by activated carbon and natural date pits.

Adsorbents	Langmuir parameters			Freundlich parameters		
	k (L/mg)	Q_e (mg/g)	R^2	1/n	K_F	R^2
N.D.P	0.267	46	0.99	0.32	11.76	0.94
D.P. 300°C	0.25	250	0.99	0.31	63.5	0.69
D.P. 400°C	0,175	434.78	0,99	0,19	163.5	0,99
D.P. 450°C	0.151	416.66	0.99	0.26	114.68	0.96
D.P. 500°C	0.225	357.14	0.99	0.211	124	0.97

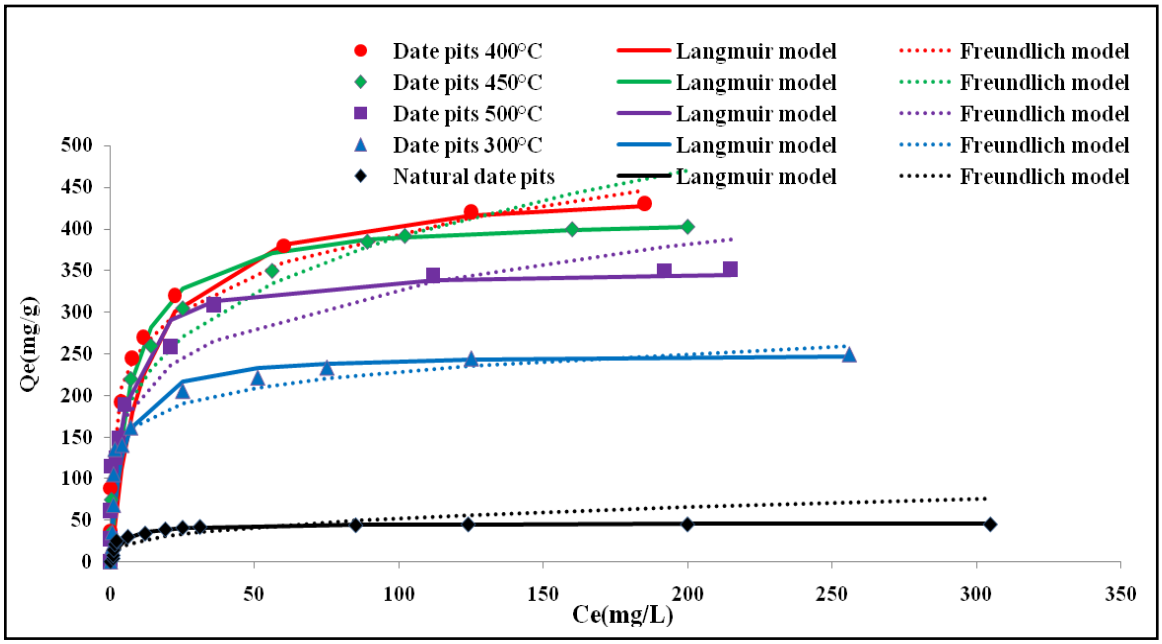

Figure 10. Modeling of adsorption isotherms of MO on raw date pits and activated carbon samples at 25°C [symbols: experiments; solid lines: Langmuir model; Broken lines: Freundlich model].

Table 4 shows a comparison of maximum monolayer adsorption capacities of MO on various adsorbents reported in the literature. From table, it was found that the activated carbon from date pits studied had a relatively high adsorption capacity toward MO.

Table 4: Maximum monolayer adsorption capacities of Mehtyl orange (MO) on various adsorbents.

Adsorbents	Q_m(mg g^{-1})	Reference
PAC-HNO3	384.62	[55]
Activated Carbon from *Phragmites australis*	238.10	[56]
Multiwalled carbon nanotubes	52.86	[57]
Activated Carbon drived from pine cone	404.42	[58]
Calcined Lapindovolcanic mud	333.3	[59]
Nanoporous core-shell Cu@Cu_2Onanocmposite	344.84	[60]
Chitosan	34.83	[61]
layered double hydroxides	285	[62]
Activated carbon from date pits at 400°C	434.78	This study

Conclusion

Activated carbons were prepared at different activation temperatures (300, 400, 450, 500°C) of date pits in a muffle furnace with zinc chloride impregnation ratios (2:1) for 2 h. The differences in physical and chemical characteristics and adsorptive properties of the four carbons were systematically studied. These results suggested that:

-The activated carbons prepared by $ZnCl_2$ at 400°C exhibited higher values of the BET surface area and total pore volume. The surface area and pores volume reached about 1380 m^2/g and 0.9cm^3/g respectively.

-Scanning electron microscopy showed the development of pores after activation.

-The textural characteristics and surface functional groups of the derived activated carbons were strongly dependent on activation temperature.

-It suggest the practical feasibility of temperature (400°C) activation of date pits, which produces high quality activated carbons with high surface area and favorable acidic surface functional groups.

The all samples were used for the removal of methyl orange. The main conclusions are as follows:

-The maximum adsorption of MO onto all adsorbent was obtained at pH 3.5 and contact time 6 hours.

-The kinetic modeling of the MO adsorption onto all adsorbents well followed the pseudo-second order rate model with the correlation coefficients of higher than 0.99.

-Adsorption behavior is described by a monolayer Langmuir type isotherms for all samples.

References

1. Gonzalez –Garcia, P., Centeno, T., Urones-Garrot, E., Avila-Brande, D., Otero-Diaz, L. C., *Appl. Surf. Sci.* 265 (2013) 731.
2. Bagheri, N., Abedi, J., *Chem Eng Res Des.* 87 (2009) 1059.
3. Njoku, V. O., Hameed, B. H., *Chem. Eng. J.* 173 (2011) 391.
4. Yang, J., Qiu, J., *Chem. Eng. J.* 165 (2010) 209.
5. Vernersson, T., Bonelli, P. R., Cerrella, E. G., Cukierman, A. L., *Bioresour. Technol*. 83 (2002) 95.
6. Cunliffe, A., Williams, P. *Energy. Fuels*, 13 (1999) 166.
7. Caturla, F., Molina-Sabio, M., Rodríguez-Reinoso, F., *Carbon*, 29 (1991) 999.
8. Ugurlu, M., Gurses, A., Acikyildiz, M., *Microporous Mesoporous Mater*. 111 (2008) 228.
9. Donald, J., Otsuka, Y., Xu, C., *Mater Lett*. 65 (2011) 744.
10. Nieto-Delgado, C., Rangel-Mendez, J. R., *Ind. Crops Prod*. 34 (2011) 1528.
11. Hu, C., He, J. Z. S., Luo, Z., Cen, K., *Fuel Process Technol*. 90 (2009) 812.
12. Foo, K. Y., Hameed, B. H. *Desalination*, 275 (2011) 302.
13. Foo, K. Y., Hameed, B. H. Eng. J., 187 (2012) 53.
14. Xiao, H., Peng, H., Deng, S., Yang, X., Zhang, Y., Li, Y., *Bioresour. Technol*. 111 (2012) 127.
15. Muthanna, J. A., Theydan, S. K., *Chem. Eng. J.*, 214 (2013) 310.
16. Ould-Idriss, A., Stitou, M., Cuerda-Correa, E. M., Fernández-González, C., Macías-García, A., Alexandre-Franco, M. F., Gómez-Serrano, V., *Fuel processing Technol*. 92 (2011) 261.
17. Liu, H., Wang, X., Zhai, I., Zhang, J., Chenglu, Z., Bao, N., Cheng, C., *Chem. Eng. J.* 209 (2012) 155.
18. Hadoun, H., Sadaoui, Z., Souami, N., Sahel, D., Toumert, I., *Appl Surf Sci*. 280 (2013) 1.
19. Wilson, K., Yang, H., Seo, C. W., Marshall, W. E., *Bioresour. Technol*. 97 (2006) 2266.
20. Girgis, B. S., Yunis, S. S., Soliman, A. M., *Mater. Lett*. 57 (2002) 164.
21. Mahmoudi, K., Hamdi, N., Kriaa, A., Srasra, E., *Russ. J. Phys. Chem. A*, 86 (2012) 1294.
22. Prakash, Kumara, B. G., Shivakamy, K., Mirandaa, L. R., Velan, M., *J. Hazard. Mater*. B, 136 (2006) 922.
23. Matos, J., Nahas, C., Rojas, L., Rosales, M. *J. Hazard. Mater.* 196 (2011) 360.
24. Valix, M., Cheung, W. H., Mckay, G., *Chemosphere*, 56 (2004) 493.
25. Kalderis, D., Bethanis, S., Paraskeva, P., Diamadopoulos, E., *Bioresour. Technol.* 99 (2008) 6809.
26. Fierro, V., Muniz, G., Basta, A. H., El-Saied, H., Celzard, A., *J. Hazard. Mater,* 181 (2010) 27.
27. Lussier, M. G., Shull, J. C., Miller, D. J,. *Carbon*, 32 (1994) 1493.
28. Purnomo, C. W., Salim, C., Hinode, H., *J. Anal. Appl. Pyrolysis*, 91 (2011) 257.
29. Soares, Maia, D. A., Sapag, K., Toso, J.P., López, R. H., Azevedo, D. C. S., Cavalcante, J. C. L., Zgrablich G., *Microporous Mesoporous Mater*., 134 (2010) 181.
30. Baccar, R., Bouzid, J., Feki, M., Montiel, A., *J. Hazard. Mater.* 162 (2009) 1522.
31. Yeddou, A. R., Nadjemi, B., Halet, F., Ould-Dris, A., Capart, R. Min. Eng. 23 (2010) 32.

32. Bouchelta, C., Medjram, M. S., Bertrand, O., Bellat, J. P., *J. Anal Appl Pyrolysis*, 82 (2008) 70.
33. Hazourli, S., Ziati, M., Hazourli, A. *Phy. Proced*. 2 (2009) 1039.
34. Belhachemi, M., Rios, R. V. R. A., Addoun, F., Silvestre-Albero, J., Sepulveda-Escribano, A., Rodriguez-Reinoso, F. , *J. Anal. Appl. Pyrolysis*, 86 (2009) 168.
35. Banat, F., Al-Asheh, S., Al-Makhadmeh, L., *Process Biochem*,. 39 (2003) 193.
36. Dastgheib, S. A., Rockstraw, D. A., *Carbon*, 40 (2002) 1843.
37. Rodríguez-Reinoso, F., *Pure Appl. Chem*. 61 (1989) 1859.
38. Dinesh, M., Ankur, S., Singh, V.K., Alexandre-Franco, M., Pittman, C.U., *Chem. Eng. J.* 172 (2011) 1111.
39. Noh, J. S., Schwarz, J. A., *J. Colloid. Interf. Sci*. 130 (1989) 157.
40. Boehm, H. P., *Adv Catal*. 16 (1966) 179.
41. Boehm, H. P., *Carbon*, 32 (1944) 759.
42. Papier, E., Li, S., Donnet, J. B., *Carbon*, 25 (1987) 243.
43. Ouasif, H., Yousfi, S., Bouamrani, M.L., El Kouali, M., Benmokhtar, S., Talbi M., *J. Mater. Environ. Sci.* 4 (1) (2013) 1.
44. Umoren, S. A., Etim, U. J., Israel, A. U., *J. Mater. Environ. Sci.* 4 (1) (2013) 75.
45. Langmuir., *Journal of the American Chemical Society*, 38 (1916) 2221.
46. Freundlich, H.M.F., *J. Phys. Chem*. 57 (1906) 385.
47. Lagergren, S. Kungliga Svenska Vetenskapsakademiens., *Handlingar*, 24 (1989) 1.
48. Ho, Y.S., McKay G., *Process Safety and Environmental Protection*, 76 (1998) 183.
49. Chang, C. F., Chang, C. Y., Tien, W. T., *J. Colloid Interf. Sci*. 232 (2000) 45.
50. Buczek, B., Swiatkowski, A., Zietek, S., Trznadel, B. J., *Fuel*, 79 (2000) 1247.
51. Pradhan, B. K., Sandle, N.K., *Carbon*, 37 (1999) 1323.
52. Lua, A. C., Yang, T., *J. Colloid. Interf. Sci*. 290 (2005) 505.
53. El-Sharkawy, E. A., Soliman, A. Y., Al-Amer, K. M., *J. Colloid Interf. Sci*. 310 (2007) 498.
54. Rodríguez, A., García J., Ovejero, G., Mestanza, M., *J. Hazard. Mater*. 172 (2009) 1311.
55. Do, M.H., Phan, N.H., Nguyen, T.D., Pham, T.T.S., Nguyen, V.K., VU, T.T.T., Nguyen, T.K.P., *Chemosphere*, 85 (2011) 1269.
56. Chen, S., Zhang, J., Zhang, C., Yue, Q., Li,T., Li, C., *Desalination*, 252 (2010) 149.
57. Yao, Y., He, B., Xu, F., Chen, X., *Chem. Eng. J*. 170 (2011) 82.
58. Samarghandi, M.R., Hadi, M., Moayedi, S., Askari, F.B. Iran., *J. Environ. Health Sci. Eng.* 6 (2009) 285.
59. Jalil, A.A., Triwahyonob, S., Adama, S.H., Rahima, N.D., Aziza, M.A., Hairom, N.H., Razalia, N.A.M., Abidina, M.A.Z., Mohamadia M.K.A., *J. Hazard. Mater.* 181 (2010) 755.
60. Kou, T., Wang, Y., Zhang, C., Sun, J., Zhang, Z., *Chem. Eng. J*. 223 (2013) 76.
61. Saha, T.K., Bhoumik, N.C., Karmaker, S. Ahmed, M.G., Ichikawa, H., Fukumori,Y., *J. Water Resour. Prot.* 2 (2010) 898.
62. Zhe-Ming, N., Sheng-Jie, X., Li-Geng W., Fang-Fang, X., Guo-Xiang, P., *J. Colloid Interf. Sci.* 316 (2007) 284.